

¹⁴N NMR Evidence for Initial Production of NH₃ Accompanied by Alcohol from the Hydrolysis of Ethylamine and Butylamine in Supercritical Water

Ken Yoshida, *¹ Haruka Yoshioka, ¹ Natsuko Ushigusa, ¹ and Masaru Nakahara²

¹*Department of Applied Chemistry, Graduate School of Technology, Industrial and Social Sciences, Tokushima University, 2-1, Minamijousanjima-cho, Tokushima, 770-8506, Japan*

²*Institute for Chemical Research, Gokasho, Uji, Kyoto University, 611-0011, Japan*

E-mail: yoshida.ken@tokushima-u.ac.jp

1 A ¹⁴N and ¹H NMR spectroscopic study was carried out
2 to shed light on the microscopic aspects of the reaction of
3 model alkylamines at a supercritical temperature of 400 °C.
4 It is disclosed that NH₃ and ROH (R = CH₃CH₂ and CH₃
5 (CH₂)₃) are initially produced from the hydrolysis of
6 ethylamine and butylamine, respectively. When the water
7 density is doubled from 0.2 g cm⁻³, the pseudo-first-order
8 reaction rate is markedly enhanced beyond the linear
9 response. It suggests that the transition state of C-N bond
10 cleavage is in a dipolar (ionic) state that can be more
11 stabilized due to the many-body solvation by highly polar
12 water molecules at a higher density.

13 **Keywords:** Film Forming Amines, Supercritical Water,
14 **Nuclear Magnetic Resonance**

15 Achieving further growth of renewable energy has
16 become an urgent issue to protect the global environment. For
17 the implementation of variable renewable energy (VRE) in
18 the power supply, an efficient combination with the
19 traditional fossil power is practically indispensable to secure
20 the safe and stable supply. Frequent shutting down and
21 starting up of a fossil plant for tuning the supply are
22 demanding operation from the viewpoint of the equipment
23 maintenance because undesirable gaseous corrosives as
24 oxygen and carbon dioxide can be brought into the steam-
25 water cycle. Thus, there have been increasing demands for
26 effective corrosion inhibitors. For the purpose, film forming
27 amines (FFA) have been employed in recent years, and more
28 fundamental research needs for this issue are emphasized,
29 e.g., by The International Association for the Properties of
30 Water and Steam (IAPWS); Technical Guidance Documents
31 (TGDs) on the application of FFA in steam power plants¹ and
32 industrial steam generators.² By introducing FFA, a
33 hydrophobic film is formed on the inner surface of tubes for
34 steam-water cycles and it is thought that the film can hinder
35 the contact of corrosives and water to the tube materials.^{3,4}

36 One of the major concerns about the application of FFA
37 arises from lack of information about the stability of FFA in
38 such severe high-temperature high-pressure conditions and
39 that about product species when FFA degrade. In particular,
40 organic acids are most undesirable products. Moed et al.
41 reported that organic acids were produced from low
42 molecular weight amines (so-called alkalizing amines used to
43 keep the circulating water in a basic condition) in the
44 temperature range of 500–560 °C.⁵ An extremely low amount
45 of organic acids on the order of 100 ppb or less were reported
46 to be produced from the 10-ppm reactant. While there have
47 also been reported observations of the decomposition of low-
48 molecular-weight alkalizing amines under hydrothermal
49 conditions including those at lower temperatures of a nuclear

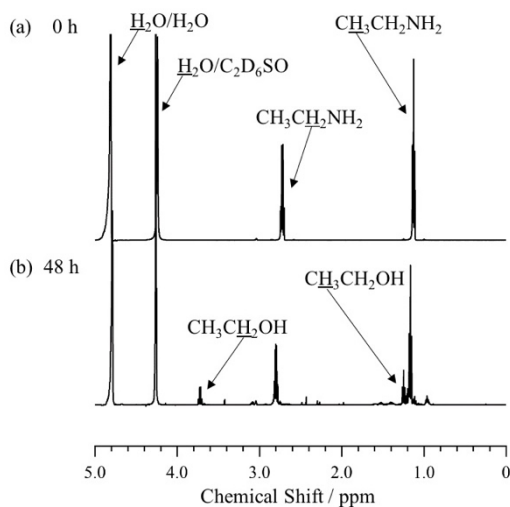
50 reactor around 300 °C,^{6–8} the reaction paths, in particular the
51 initial steps, have not been clarified yet. Since there are
52 involved a wide range of thermodynamic states in a steam-
53 water cycle in the power plant, it is essential to clarify the
54 reaction pathways of FFA to confirm the effectiveness and
55 safety.

56 Ethylamine (EtA, 70 vol% aqueous solution, Nacalai
57 Tesque) and butylamine (BuA, ≥99.0%) were used without
58 further purification. Solvent water was purified using a Milli-
59 Q Gradient A-10 system (Merck Millipore). In this study,
60 ordinary water H₂O was used instead of deuterated water D₂O
61 to avoid the exchange of hydrogens of alkyl chains with
62 deuteriums; this exchange occurs at high temperatures as
63 reported elsewhere.^{9,10} The solution of EtA, prepared at 1.0
64 mol dm⁻³ under ambient conditions, was injected into a
65 quartz glass tube reactor (2.0 mm i.d. and 4.0 mm o.d.), the
66 air in the gaseous phase was exchanged with argon so that the
67 reaction can be free from O₂ from the air, and the tube was
68 sealed with a gas burner. The density at a supercritical
69 temperature was controlled by adjusting the ratio of the
70 solution injected into the quartz tube reactor under ambient
71 conditions to the inner volume of the reactor; e.g., the
72 supercritical water density is 0.2 g cm⁻³ when the ratio is 0.2.
73 High temperature reaction was carried out by putting the
74 quartz tube reactor into an electronic furnace preheated to a
75 reaction temperature; the temperature was controlled within
76 ± 1 °C. After a reaction time, the reactor tube was taken out
77 of the electric furnace and put into a water bath to quench the
78 reaction.

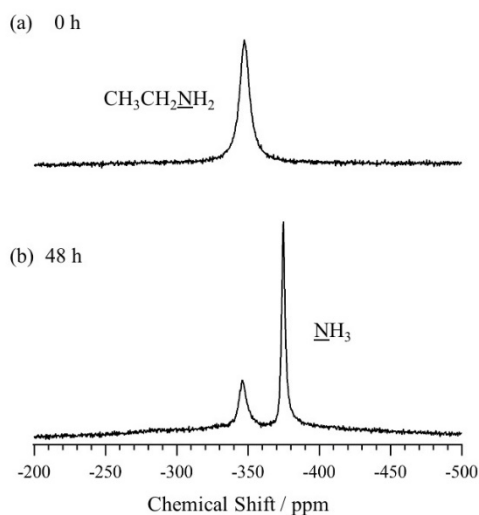
79 The reaction products were monitored using ¹H and ¹⁴N
80 NMR spectroscopy with a JEOL ECA500W spectrometer.
81 For a ¹H NMR measurement, a quartz tube reactor was placed
82 into a 5-mm NMR sample tube (5.0 mm o.d. and 4.2 mm i.d.).
83 For a ¹⁴N NMR, three reactor tubes were placed in a 10-mm
84 NMR sample tube (10.0 mm o.d. and 9.0 mm i.d.). The space
85 between the quartz tube(s) and the NMR sample tube was
86 filled with DMSO-d₆ used for ²H locking. The ¹H signal of
87 water was suppressed by DANTE presaturation.¹¹ The ¹H
88 chemical shift was externally referenced to the methyl proton
89 of sodium 3-(Trimethylsilyl)propionate-2,2,3,3-d₄ (TMSP-
90 d₄, 0.000 ppm) in an aqueous solution which was placed in
91 the same geometry as that of the aqueous amine solution. The
92 ¹⁴N NMR (36 MHz at 11.7 T magnet) spectra were measured
93 using a probe for the low-frequency nuclei (JEOL T10L). The
94 ¹H and ¹⁴N signals were accumulated for 16 and 4096 times,
95 respectively, to attain a good signal-to-noise ratio.

96 The gas NMR was measured for ¹H and ¹³C nuclei by
97 placing the sample tube upside down; the inner diameter of
98 2.0 mm is narrow enough to keep the liquid phase remaining

1 in the upper side due to the surface tension during the
 2 measurement.¹⁰ The ¹H and ¹³C signals were accumulated for
 3 16 and 16384 times, respectively. In the measurement of the
 4 gas phase, liquid products on the inside wall of the quartz tube
 5 were observed in addition to the gaseous products. The
 6 gaseous products were distinguished from liquid ones
 7 according to the diffusivity (difference in 3 orders of
 8 magnitude in self-diffusion coefficients between gas and
 9 liquid phases) measured by using the pulsed-field-gradient
 10 spin-echo method.^{12, 13}



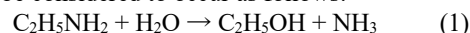
11
 12 **Figure 1.** ¹H NMR spectra of the aqueous solution of EtA (a)
 13 before the supercritical water reaction (reaction time of 0 h) and
 14 (b) treated at 400 °C for 48 h at 0.20 g cm⁻³. In (a) the peaks at
 15 1.16 and 2.80 ppm are assigned to the methyl and methylene
 16 protons of the reactant EtA, respectively, the peaks at 4.79 ppm
 17 (distorted by water suppression) to the solvent water, and the
 18 peak at 4.26 ppm to the impurity water in DMSO-d₆. In (b) the
 19 peaks at 1.25 and 3.72 ppm are assigned to the methyl and
 20 methylene protons of the product EtOH, respectively.



21
 22 **Figure 2.** ¹⁴N NMR spectra of the aqueous solution of EtA (a)
 23 before the supercritical water reaction (reaction time of 0 h) and

24 (b) treated at 400 °C for 48 h at 0.20 g cm⁻³. The peaks at -346
 25 and -375 ppm are assigned to EtA and NH₃, respectively.

26 Quantitative determination of the reaction products as
 27 functions of time and conditions is the most important first
 28 step for the kinetic study. Figure 1 shows how the ¹H NMR
 29 spectra changes after a 48-h reaction at a supercritical
 30 temperature of 400 °C and at a density of 0.2 g cm⁻³, and how
 31 the observed signals are assigned. It is found that EtOH is
 32 initially produced, so the hydrolysis of the N-H bond of EtA
 33 can be considered to occur as follows:



35 To make sure this reaction pathway, we need to confirm the
 36 counter species of C₂H₅OH, i.e., NH₃ that cannot be detected
 37 however by ¹H NMR due to the rapid proton exchange. For
 38 the purpose, we applied the ¹⁴N NMR spectroscopy by
 39 overcoming the low sensitivity. Figure 2 shows the ¹⁴N NMR
 40 spectra taken under the same reaction conditions as those of
 41 Figure 1. After the reaction, there is clearly observed a signal
 42 for NH₃. The NH₃ signal is sufficiently separated for the
 43 quantitative analysis from that for the amino residue of EtA;
 44 the two signals are deconvoluted into two Lorentzian peaks.

45 Now let us examine whether any other reactions take
 46 place in addition to eq 1. As seen in Figure 1b, there are
 47 various weak peaks besides the EtOH ones. This indicates
 48 that the hydrothermal reaction expressed by eq 1 is initially
 49 dominant but not exclusive during the long reaction time. To
 50 understand this more, we show the time evolution of the
 51 concentration of the reactant and products of EtA treated at
 52 400 °C for 72 h at 0.20 g cm⁻³ in Figure 3. When we pay
 53 attention only to the reactant EtA and one of the products NH₃
 54 we can see the reaction of the amino moiety is rather simple.
 55 The amounts of EtA determined by the ¹H and ¹⁴N NMR
 56 spectroscopic methods coincide with each other within the
 57 experimental uncertainties (~10%). The decrease of the
 58 reactant EtA and the increase of NH₃ are approximately in
 59 one-to-one correspondence; the sum of EtA and NH₃
 60 corresponds to the mass balance determined by ¹⁴N NMR,
 61 which is roughly kept at unity. A slight decrease in the mass
 62 balance, ranging to 10%–20%, can be ascribed to the
 63 adsorption of amino residue of EtA onto the inner surface of
 64 the quartz tube. The reasonably good mass balance with
 65 respect to ¹⁴N indicates that eq 1 dominates the amino group
 66 reaction; there are some minor heterogeneous side-reactions
 67 as mentioned above.

68 In contrast to the amino group, the ethyl has complicated
 69 hydrothermal reaction pathways besides eq 1. Figure 1
 70 exhibits several ¹H signals besides EtOH in the liquid phase.
 71 Although at present the individual assignment is difficult due
 72 to the signal overlapping, the group assignment is possible in
 73 view of the high-field chemical shifts. There were also
 74 several unassigned signals observed in the gas phase as seen
 75 in Figure S1 in Supporting Information. We can determine
 76 the yields of the unknown (UK) products to confirm the
 77 validity of the overall mass balance under the assumption that
 78 the number of protons of a product species originating from
 79 one reactant EtA molecule is five. In the methyl-proton
 80 region (0.9–1.7 ppm) in the liquid phase, where signals
 81 overlap most severely, the amount of the intensities of methyl

1 protons of EtA and EtOH were estimated based on their
 2 methylene protons that are more separated, and the intensities
 3 of the UK peaks can be obtained by subtracting those of EtA
 4 and EtOH from the integral intensity of the whole methyl-
 5 proton region. The amounts of the UK thus determined are
 6 plotted in Figure 3. The sum of the reactant and the products
 7 are shown as the ^1H mass balance. The mass balance is
 8 approximately kept unity as in the case of the ^{14}N mass
 9 balance, which verifies the validity of the assumption used to
 10 quantify UK. This means that the conversion from less
 11 exchangeable protons, such as methyl, to the exchangeable
 12 one, such as hydroxyl, is not significant and almost negligible
 13 in the analysis of the product yields. The UK in both phases
 14 increase until 48 h, and after that, the UK in the liquid phase
 15 decrease and those in the gas phase increase, showing that
 16 the products in the liquid phase are intermediate ones that are
 17 subsequently converted into gaseous ones with the mass
 18 balance kept. For further assignment of the UK, an intensive,
 19 high sensitivity ^{13}C NMR can be done with an enriched
 20 sample and/or two-dimensional measurements are needed.
 21

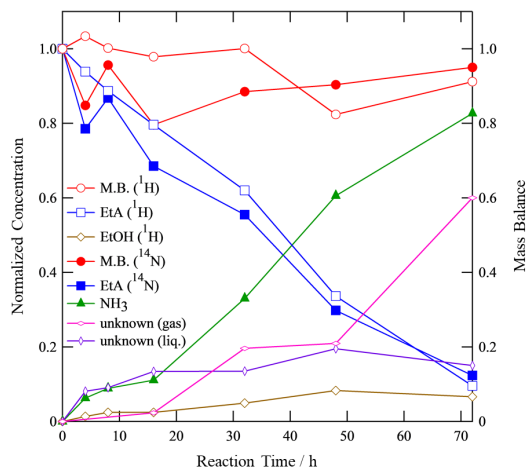


Figure 3. Time evolutions of the concentrations of the reactant and products for the reactions of ethylamine at 400 °C and at 0.20 g cm⁻³. The vertical axis on the left shows the normalized concentration, and that on the right shows the mass balance. The normalized concentration denotes the concentration of the compound of interest divided by the initial substrate concentration. The mass balance denotes the ratio of the sum of the amount of nitrogen or proton atoms in the reactant and the products detected by ^{14}N or ^1H NMR at each reaction time divided by the amount of the corresponding nucleus of the reactant in the beginning of the reaction.

34 Now let us examine the effect of the water density. The
 35 time evolutions of the reactant and products at 0.40 g cm⁻³
 36 are shown in Figure S2 in Supporting Information, for which
 37 the reaction temperature and the molality of EtA are set to be
 38 the same as those for Figure 3. It is seen that the decrease of
 39 EtA and the increase of NH₃ become significantly faster
 40 when the water density is doubled. For the quantitative
 41 comparison, we fitted the concentration of ethylamine to
 42 pseudo-first-order kinetics, $d[\text{EtA}]/dt = -k[\text{EtA}]$, where
 43

44 [EtA] is the concentration of ethylamine and k is the pseudo-
 45 first-order reaction rate constant. The k values thus
 46 determined at 0.20 and 0.40 g cm⁻³ are $(6.6 \pm 0.7) \times 10^{-6}$ and
 47 $(3.4 \pm 0.5) \times 10^{-5} \text{ s}^{-1}$, respectively. The rate is enhanced by a
 48 factor of (5 ± 2) , much larger than the density increase. The
 49 increase of the rate constant overwhelms the proportionality
 50 to the water density, implying that the crowding of water
 51 molecules around the reactant promotes the cleavage of the
 52 amino residue from the reactant amine in the hydrolysis
 53 reaction. The acceleration due to water suggests that the
 54 barrier-crossing transition state is in a polar or ionic state,
 55 which can be more stabilized by electrostatic interactions at
 56 higher densities. Further comprehensive theoretical and
 57 experimental investigations are required concerning the
 58 effect of size and hydrophilicity/hydrophobicity of functional
 59 groups in the reactant amines.
 60

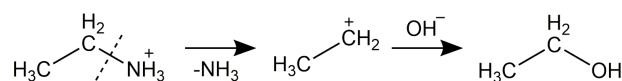


Figure 4. Proposed mechanism of the hydrolysis C-N bond cleavage of EtA in supercritical water.

63 The dramatic influence of the supercritical water density
 64 found here leads us to such a mechanism for the hydrolytic
 65 cleavage of the C-N bond of EtA in supercritical water as
 66 illustrated in Figure 4. First, the amino group of EtA is
 67 protonated through the contact with water molecules and then
 68 the C-N bond is polarized and broken to release NH₃. The
 69 fragment CH₃-CH₂⁺ immediately binds to a neighboring
 70 hydroxide ion to produce CH₃CH₂OH; otherwise, it binds
 71 back to -NH₃⁺ as the reverse reaction. In this mechanism, the
 72 elongation of the C-N bond to produce the unstable fragment
 73 CH₃-CH₂⁺ is the rate-determining step. The assumption of an
 74 ionic species in the transition state is consistent with the
 75 experimental observation that the reaction is dramatically
 76 accelerated by the increase in the water density; the ionic
 77 species, as well as polar ones, will be more stabilized by
 78 lowering the solvation free energy at a higher water density
 79 in supercritical states.¹⁴ Elimination of NH₃ from neutral EtA
 80 is unlikely to occur because the counter species ethene is not
 81 observed in the gas-phase ^1H and ^{13}C NMR spectra (Figure
 82 S1 in Supporting Information). It is plausible that the UK
 83 species are produced by the reaction of ethanol. The reaction
 84 of ethanol in supercritical water in a quartz glass reactor tube
 85 was reported by Arita et al.¹⁵ and the major product species
 86 reported were hydrogen, methane, ethane, and acetaldehyde,
 87 none of which are observed in our present study as seen in
 88 Figure S1. The difference in the product species could be
 89 attributed to the basicity, and an investigation of this point
 90 will be of particular interest in relation to steam-water cycles
 91 whose circulating water is kept being basic for controlling
 92 corrosion. For FFA applications, the important issue is to
 93 what extent the products contain acidic species. We measured
 94 the pH value of the aqueous phase at room temperature after
 95 the high-temperature reaction. The pH values for the sample
 96 treated for 4, 8, and 16 h at 400 °C and at 0.40 g cm⁻³ were
 97 11.9, 12.0, and 10.7, respectively. While there observed a

1 slight downward shift at 16 h, the pH value remains
 2 satisfactorily in basic conditions. This means that the
 3 production of acidic species is, if any, not the dominant
 4 determining factor of the pH due to the overwhelming NH₃.
 5 Thus, the NH₃ production is efficient for suppressing the
 6 corrosion through the pH control.

7 Now let us examine the effect of the alkyl chain length
 8 of the reactant amines. To the end, we examined the
 9 decomposition of butylamine (BuA) at 400 °C and at 0.20 g
 10 cm⁻³ for the comparison with that of EtA described above.
 11 Examination by ¹H NMR showed that BuA decomposes
 12 about three times faster than EtA; a pseudo-first-order
 13 reaction rate constant for BuA is $(2.0 \pm 0.4) \times 10^{-5} \text{ s}^{-1}$. In the
 14 product species, butanol (BuOH) was observed as the
 15 hydrolysis product in parallel with eq 1; the amount of
 16 produced BuOH was smaller by 10%–30% than that of the
 17 consumed reactant BuA as in the case of EtA. The similarity
 18 in the product distribution between EtA and BuA suggests
 19 that the reaction pattern like eq 1 is common to alkylamines
 20 whatever the chain length is. In supercritical states, there
 21 would be more microscopic inhomogeneity of hydrophilic
 22 and hydrophobic moieties of alkylamines when the alkyl
 23 chains are longer.¹⁶ In supercritical states where there is
 24 larger density inhomogeneity, hydrophilic and hydrophobic
 25 moieties could enhance localization of reactant water
 26 molecules around hydrophilic amino residues, leading to the
 27 stabilization of the transition state. To have molecular
 28 insights into the reaction mechanism of the hydrolysis of
 29 amines in supercritical conditions, we need to do a more
 30 comprehensive and systematic kinetic analysis as a function
 31 of key parameters such as the alkyl chain length and a
 32 reactant concentration.

33
 34 This study is supported by Grants-in-Aid for Scientific
 35 Research (Nos. 17K05754 and 20K05433) from the Japan
 36 Society for the Promotion of Science (JSPS). K. Y. is grateful
 37 for the grant from IMRA JAPAN Co., Ltd as a supplementary
 38 prize of the 3rd IMRA JAPAN Award. Mr. Shintaro Mori,
 39 Mr. Kazuyoshi Uchida, and Mr. Masakazu Koizumi at Kurita
 40 Water Industries Ltd. are thanked for helpful discussions.

41
 42 Supporting Information is available on
 43 http://dx.doi.org/10.1246/cl.*****.

44 References and Notes

- 45
 46 1 International Association for the Properties of Water and Steam,
 47 *Application of Film Forming Substances in Fossil, Combined*
 48 *Cycle, and Biomass Power Plants*, Technical Guidance Document
 49 IAPWS TGD8-16, **2019**.
 50 2 International Association for the Properties of Water and Steam,
 51 *Application of Film Forming Substances in Industrial Steam*
 52 *Generators*, Technical Guidance Document IAPWS TGD11-19,
 53 **2019**.
 54 3 B. Dooley, D. Lister, *PowerPlant Chemistry* **2018**, 20, 194.
 55 4 S. Weerakul, N. Leaukosol, D. H. Lister, S. Mori, W. Hater,
 56 *Corrosion* **2020**, 76, 217.
 57 5 D. H. Moed, A. R. D. Verliefe, L. C. Rietveld, *Ind. Eng. Chem.*
 58 *Res.* **2015**, 54, 2606.
 59 6 R. Gilbert, C. Lamarre, *Can. J. Chem. Eng.* **1989**, 67, 646.
 60 7 D. Féron, I. Lambert, *J. Solution Chem.* **1992**, 21, 919.

- 61 8 M. Domae, K. Fujiwara, *J. Nucl. Sci. Technol.* **2009**, 46, 210.
 62 9 M. Kubo, T. Takizawa, C. Wakai, N. Matubayasi, M. Nakahara, *J.*
 63 *Chem. Phys.* **2004**, 121, 960.
 64 10 Y. Yasaka, K. Yoshida, C. Wakai, N. Matubayasi, M. Nakahara,
 65 *J. Phys. Chem. A* **2006**, 110, 11082.
 66 11 G. A. Morris, R. Freeman, *J. Magn. Reson. (1969)* **1978**, 29, 433.
 67 12 E. O. Stejskal, J. E. Tanner, *J. Chem. Phys.* **1965**, 42, 288.
 68 13 P. Stilbs, *Prog. Nucl. Magn. Reson. Spectrosc.* **1987**, 19, 1.
 69 14 N. Matubayasi, M. Nakahara, *J. Chem. Phys.* **2005**, 122, 074509.
 70 15 T. Arita, K. Nakahara, K. Nagami, O. Kajimoto, *Tetrahedron Lett.*
 71 **2003**, 44, 1083.
 72 16 K. Yoshida, M. Nakahara, *J. Chem. Phys.* **2019**, 150, 174505.

73
 74

1
2
3
4
5
6
7
8
9
10
11

NOTE The diagram is acceptable in a colored form. Publication of the colored G.A. is free of charge.

For publication, electronic data of the colored G.A. should be submitted. Preferred data format is EPS, PS, CDX, PPT, and TIFF.

If the data of your G.A. is "bit-mapped image" data (not "vector data"), note that its print-resolution should be 300 dpi.

You are requested to put a brief abstract (50-60 words, one paragraph style) with the graphical abstract you provided, so that readers can easily understand what the graphic shows.

Graphical Abstract	
Textual Information	
A brief abstract (required)	The reaction of alkylamines at a supercritical temperature of 400 °C was studied using a multinuclear NMR spectroscopy. It was revealed for the first time that the initial step is the hydrolysis cleavage of the C-N bond to produce ammonia. The reaction mechanism is proposed based on the effect of the water density as illustrated.
Title(required)	¹⁴ N NMR Evidence for Initial Production of NH ₃ Accompanied by Alcohol from the Hydrolysis of Ethylamine and Butylamine in Supercritical Water
Authors' Names(required)	Ken Yoshida, Haruka Yoshioka, Natsuko Ushigusa, and Masaru Nakahara
Graphical Information	
<p><Please insert your Graphical Abstract: The size is limited within 100 mm width and 30 mm height, or 48 mm square>(required)</p> 